Finite element model of the human neck during omni-directional impacts

Part I. Kinematics and injury

Bertrand Fréchède* — Nicolas Bertholon*'**
Jean-Yves Le Coz — Francois Lavaste* — Wafa Skalli***

** Labo. de Biomécanique, ENSAM, 151 Bd. de l'Hôpital, F-75013 Paris*

{francois.lavaste, wafa.skalli @paris.ensam.fr

*** Labo. d'accidentologie, de biomécanique et d'études du comportement humain PSA Peugeot-Citroën Renault, 132 rue des Suisses, F-92000 Nanterre*

b.frechede@unsw.edu.au ; nicolas.bertholon@mpsa.com ; jean-yves.le-coz@renault.com

ABSTRACT. *A 3D Finite Element model was developed under the FE code Radioss, to explore the mechanisms of injury occurring during various kinds of impacts. It represents the head and neck of a 50th percentile human seated in a reference position. It includes a volumic representation of the head, cervical vertebras, intervertebral discs, muscles and soft tissues. Contacts are taken into account between articular facets as well as between spinous processes. The kinematical behaviour of the model was evaluated omni-directionally for various impacts, using published experimental results of head and vertebral 3D motions and accelerations, obtained both on cadavers and volunteers. The model's ability to reproduce injury mechanisms was also assessed; its behaviour was compared to available experimental injury assessment data, therefore allowing to define local injury criteria.*

RÉSUMÉ. *Un modèle éléments-finis 3D du cou humain a été développé sous le code EF Radioss afin d'explorer les mécanismes lésionnels dus à divers types de chocs. Il représente le complexe tête/cou d'un être humain du 50e percentile assis en position de référence. Il inclut une modélisation volumique de la tête, des vertèbres cervicales, des disques intervertébraux, des muscles et tissus mous du cou, ainsi qu'une prise en compte des contacts entre les facettes articulaires et les processus épineux. Le comportement cinématique du modèle a été évalué de manière omni-directionnelle pour différents chocs. A cet effet, des résultats expérimentaux obtenus sur volontaires ou cadavres et disponibles dans la littérature ont été utilisés. Ils concernent la cinématique de la tête ou des vertèbres. La capacité du modèle à reproduire les mécanismes lésionnels a également été évaluée et comparée à des données lésionnelles expérimentales afin de définir des tolérances lésionnelles locales.*

KEYWORDS: *neck, modelling, impact, injury.*

MOTS-CLÉS : *cou, modélisation, choc, lésion.*

1. Introduction

The neck is a complex structure both from the anatomical and mechanical point of view. During automotive crashes, head motion is related to neck behaviour. Moreover neck injuries result from a complex mechanism which is not yet fully understood. In the last ten years, multi-body (De Jager *et al*., 1996) and Finite Element (Bertholon *et al*., 1998; Yang *et al*., 1998) models have been presented in the literature with increasing complexity (Hasegawa 2004; Stemper *et al*., 2004). However, these models were generally validated only for particular impact conditions and none of them was evaluated for all kinds of impact. Concerning injury, some complex multi-body or finite element models exist but they were tested mainly in axial (Yang *et al*., 1998; Halldin *et al*., 2000) or rear-end impact (Hasegawa 2004; Stemper *et al*., 2004). Thus, the objective of our study was to develop a three-dimensional finite element model describing the dynamic behaviour of the human head and neck for omnidirectional automotive accidents. We also aimed at describing an injury predictive model, *i.e*. at validating the model against experimentally observed injury mechanisms and at defining local injury tolerance values for the model, in order to use the model in a predictive way.

2. Materials and methods

2.1. *Geometry of the model*

The neck model is an improvement and part of a 50th percentile complete human body model previously developed with the FE code RADIOSS (Lizee *et al*., 1998). Geometric data for the seated subject in driving posture (Robbins *et al*., 1983) was used as a reference to derive the global position and dimension of head and neck. The head represents a Hybrid III dummy geometry. The main mechanical features of C2-T1 vertebras were taken into account, their geometric modelling as well as the contacts between them were previously described in (Dauvilliers *et al*., 1994). Each intervertebral disk from C2 to T1 was modelled together with anterior and posterior ligaments; the interspinous and flava ligaments as well as joint capsules were represented by spring-damper elements. The links between C1 and C2 and between the head and C1 were located (White *et al*., 1990) and modeled by two 3D rotational spring-damper elements. A volumic representation was chosen for soft tissues and muscles. This allowed to keep lines of action for the muscles during impacts, to better distribute mass and inertial properties of the neck and to simulate internal and external interactions. The muscles and soft tissues geometry and their relative positions were taken from physical sections of the human male cadaver from the Visible Human Project (National Library of Medicine, 1997). One section per vertebral level was chosen, scaled, and modeled. These elements were divided into one global soft tissue group and 4 muscular groups: dorsal, prevertebral, scaleni and sternocleidomastoid muscles. Finally the skin was represented by 112 membrane elements attached to the circumference of the neck (see Figure 1).

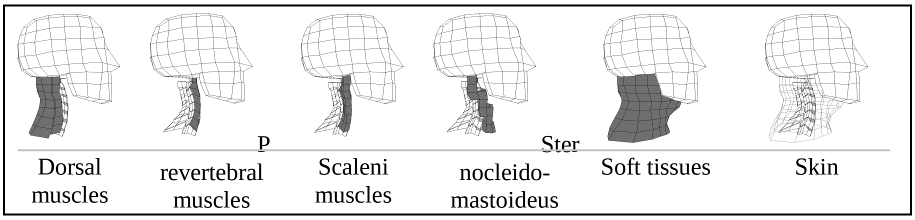

Figure 1. *Lateral views of model muscles, soft tissues and skin*

2.2. *Mechanical and inertial properties of the model*

The mechanical properties used in the model are summarized in Table 1. The vertebras and head were considered as rigid bodies. However a viscoelastic behaviour (Camacho *et al.*, 1997) was used for the head external layer of brick elements, as well as for the intervertebral disks (together with anterior and posterior ligaments). The applied viscoelastic law is based on the Boltzman model. The elastic bulk modulus K and parameters of the shear relaxation function: $G(t)=G_1+(G_0-G_1)\times e^{(-\beta t)}$ are based on the decay constant and short-time Young's modulus estimated by (Kelley *et al.*, 1983; Moroney *et al.*, 1988) – see Table 1. The static nonlinear characteristics of the upper cervical joints, taken from the literature (Goel *et al.*, 1988; Panjabi *et al.*, 1988; Watier 1997), are summarized in Figure 2. A constant rotational damping of 0.5 N.m.s/rad was chosen (Chang *et al.*, 1992).

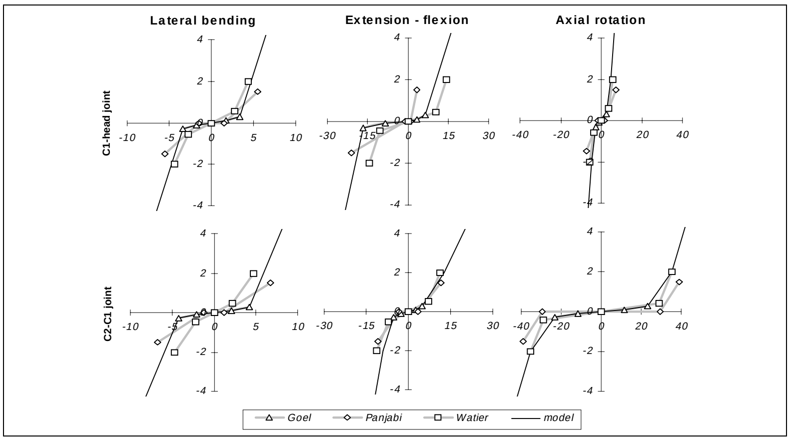

Figure 2. *Mechanical static properties of the C1-head and C2-C1 joints. Model and literature (Goel et al., 1988; Panjabi et al., 1988; Watier 1997) curves. Abscissas are the rotations (degrees) and ordinates are the moments (N.m)*

Table 1. *Model elements, mechanical behaviours and mechanical properties*

	Element (nb or *nb / level*)	Mechanical behaviour	Mechanical properties[1]
Head	Brick (304)	Rigid body or Viscoelastic	K = 3.32 MPa, G_0 = 8.20 MPa, G_l = 2.29 MPa, β = 1.591 ms^{-1}
Vertebras	Brick (*12*)	Rigid bodies	None
Intervertebral disks (with anterior and posterior ligaments)	Brick (*4*)	Viscoelastic	K = 33.33 MPa, G_0 = 7.14 MPa, G_l = 3.57 MPa, β = 0.0005 ms^{-1}
Ligaments and joint capsules	Spring-damper (*17*)	Nonlinear viscoelastic tension-only	F = f(e) see (Dauvilliers *et al.* 1994) LD = 50 N.s/m
Articular facets	Contact	Frictionless	S = 1 000 000 N/m
Spinous contacts	Contact	Frictionless	S = 2 000 000 N/m
Head-C1 joint, C1-C2 joint	3D rotational Spring-damper	Nonlinear viscoelastic	M = f(r) see Figure 2 RD = 0.5 N.m.s/rad
Muscles	Brick (200)	Anisotropic nonlinear with unloading	E = 0.3 MPa, except for traction in fiber direction where E = 2.5 MPa; E_u = 20 MPa
Soft tissues	Brick (267)	Linear with unloading	E = 0.3 MPa E_u = 20 MPa
Skin	Membrane (112)	Linear elastic	E = 5 MPa for traction E = 0.1 MPa for compression

[1]K bulk modulus; G_0 short term shear modulus; G_l long term shear modulus; β shear modulus decay constant; F force (as function of elongation); LD linear damping; S stiffness; M moment (as function of rotation); RD rotational damping; E Young's modulus; E_u unloading Young's modulus.

According to several authors (Foust *et al*., 1973; Szabo *et al*., 1996), the neck muscles reaction time is about 150 to 200 ms, therefore in a first approach only passive behaviour of muscle was taken into account. The muscles were modelled using a honeycomb law (Radioss, 2001) allowing to take into account the direction of the fibers. For each brick element of a muscular group, this direction was defined and an exponential law: $\sigma = E/\alpha\left(e^{\alpha\varepsilon} - 1\right)$ (in Goubel *et al*., 2003) was chosen, where the structural parameter α was chosen equal to 1 and the Young's modulus was taken from (Myers *et al*., 1995). For the two other orthogonal directions and for compression in fiber direction the elastic properties were taken from impact experiments on bovine muscles (McElhaney *et al*., 1965). Some of the experimental results used for validation were obtained with cadavers: To take into account the effect of postmortem time on the mechanical properties of skeletal muscle (Van Ee *et al*., 1998), an initial no-load strain of 10% was chosen for post-mortem muscle properties. The neck soft tissues were modelled as the muscles, but without fiber direction. The skin was modelled with elastic shell elements (Radioss, 2001), its characteristics coming from (Haut, 1993). The static nonlinear characteristics of the various neck ligaments were already described in (Lizee *et al*., 1998). Dynamic characteristics were found for the anterior and flavum cervical spine ligaments (Yoganandan *et al*., 1989) and the damping value of 50 N.s/m was extended to all the model ligaments. The inertial properties for the head were lumped into its rigid body and correspond to mean values found in the literature (Becker, 1972; Beier *et al*., 1980). An average density of 1000 Kg/m3 was chosen for neck soft tissues.

2.3. *Injury Criteria*

Table 2 and Table 3 present injury criteria and their associated injury levels, which were defined according to the literature. The force tolerance values proposed for functional spinal units are in axial tension (Yoganandan *et al*., 1996) and compression (McElhaney *et al*., 1983; Pintar *et al*., 1989; Nightingale *et al*., 1991; Pintar *et al*., 1995; Nightingale *et al*., 1997). The moment tolerance values proposed for functional spinal units are in flexion (Moroney *et al*., 1988; Shea *et al*., 1991), extension (Moroney *et al*., 1988) and axial torsion (Goel *et al*., 1990; Myers *et al*., 1991; Chang *et al*., 1992). Three cervical regions were considered according to these results. No literature data was found concerning shear forces and lateral bending moment for functional cervical spinal unit tolerances. It was previously observed (Yoganandan *et al*., 1989) that ligament ultimate tensile failure load increased with increasing loading rate, while this was not the case for distraction at failure. Thus tolerance values were chosen for the elongation of the ligaments (Myklebust *et al*., 1988; Yoganandan *et al*., 1998), as well as for the articular capsules (Winkelstein *et al*., 1999; Siegmund *et al*., 2000). A majority of these numerical values were obtained experimentally for old male cadavers. Some authors (Pintar *et al*., 1998) noticed that women tolerance should be lower and young males tolerance should be higher than the one proposed here.

Table 2. *Injury criteria and tolerance values for functional cervical spine units*

Axial tension force (N)	Axial compressive force (N)	Flexion moment (N.m)	Extension moment (N.m)	Axial torsion moment (N.m)
1500 (all levels)	3500 (all levels)	C0-C5: 14.0 C6-T1: 18.0	6.0	C0-C2 : 15.0 C3-T1 : 21.0

Table 3. Injury criteria and tolerance values for cervical spine ligaments

	Anterior ligaments	Posterior ligaments	Flava ligaments	Articular capsules	Interspinous ligaments
Elongation (mm)	7.3 (all levels)	6.1 (all levels)	8.0 (all levels)	8.7 (all levels)	7.3 (C2 to C5) 11.0 (C5-C6) 12.5 (C6-C7) 17.0 (C7-T1)

2.4. *Validation test database*

A set of in-vitro and global tests carried out on volunteers or on fresh cadavers was chosen. The selection of test configurations was made according to accuracy of the boundary conditions, nature of accessible results and feasibility of a reliable simulation. For each test configuration, sets of corridors were defined retaining the minimum and maximum curve envelopes or the main values and their standard deviations. Test protocols are briefly described in Table 4 for global kinematics tests and Table 5 for injury tests.

2.4.1. *Static functional spinal unit behaviour*

In vitro tests (Watier, 1997) on C7-T1 to C2-C3 functional spinal units were selected. 3D rotations under three pure moments (flexion-extension, lateral bending and axial torsion) were measured and compared to simulation results in terms of principal and coupled motion, with the lower vertebra fixed and the load applied to the upper vertebra.

2.4.2. *Head and neck kinematics*

The Naval BioDynamics Laboratory (Ewing *et al*., 1976; Dauvilliers *et al*., 1994) tests were used, where the kinematics of the head and of the first thoracic vertebra were measured for various impacts. In rear impacts without headrest, similar tests on volunteers and cadavers were selected (Kallieris *et al*., 1996; Prasad *et al*., 1997), as well as tests assessing the local relative 3D motion of various vertebras (Bertholon *et al*., 2000). To simulate these tests the linear speeds obtained on the subjects at vertebra T1 or on the sled were imposed on the model at T1. The rotation speeds were imposed when available (Bertholon *et al*., 2000) or the T1 rotation was controlled by a calibrated 3D spring (Thunnissen *et al*., 1995). All head kinematics data available were selected to evaluate the model (Table 5). For the validation simulations the mass of the instrumentation worn by subjects was taken into account.

2.4.3. *Injury tests*

Results of axial loading tests on cervical spines (Nightingale *et al*., 1991) were used. In these tests, changes in end condition produced significant and repeatable changes in mechanical responses and injury mechanisms. To simulate these tests, an axial occiput velocity was imposed with T1 vertebra fixed and the three end conditions were imposed on the occiput. (Nightingale *et al*., 1997) also studied dynamic responses of the cervical spine during head impacts. Injuries to the cervical spine were found for 5 of the 10 specimens tested with rigid impact surface. To simulate these tests, initial velocity of the head and cervical spine model was imposed with added mass and end condition (axial translation only) on T1 vertebra. The head impacted a rigid surface with three different angles. (Myers *et al*., 1991) experimentally reproduced upper and lower cervical spine injuries due to dynamic pure torsion. To simulate these tests, pure axial rotational velocity was imposed on occiput or on C2 vertebra with T1 vertebra fixed. For these three sets of tests, mechanical model responses and level of model injury criteria were measured (Table 5). The Heidelberg lesional tests (Wismans *et al*., 1987) were also used, reproducing the NBDL frontal 15g volunteer tests with cadavers.

Table 4. *Kinematics test conditions*

Reference	N° of subjects	Direction	Severity(1)	Validation data(1)
(Dauvilliers *et al.* 1994)	10 volunteers	Frontal	15 g, 60 km/h	Dx, Dz, Ry, Ax, Az, AAy
(Ewing *et al.* 1976)	77 volunteers	Frontal	3 kinds of impact onset, accelerations from 6g to 15g.	Peak values only for RA, AAy, Avy
(Dauvilliers *et al.* 1994)	12 volunteers	Lateral	7 g, 25 km/h	Dx, Dy, Dz, Rx, Ry, Rz, Ax, Ay, Az, AAx, AAy, AAz
(Dauvilliers *et al.* 1994)	12 volunteers	Oblique	10 g, 50 km/h	Dx, Dy, Dz, Rx, Ry, Rz, Ax, Ay, Az, AAx, AAy, AAz
(Bertholon *et al.* 2000)	6 cadavers	Rear-end	3 g, 11 km/h	Dx, Dz, Ry, Ax, Az, AAy
(Prasad *et al.* 1997)	1 volunteer & 2 cadavers	Rear-end	5 g, 16 km/h	Ry, Ax, Az
(Prasad *et al.* 1997), (Kallieris *et al.* 1996)	4 cadavers	Rear-end	7 g, 25 km/h	Dx, Dz, Ry, RA, AAy

(1) Dx, Dy, Dz displacements of the head anatomic center (or head CoG for rear-end impacts) from T1 in the laboratory reference; Rx, Ry, Rz head rotations calculated using Bryant's angles of the head anatomic reference with respect to the laboratory reference; Ax, Ay, Az accelerations of the head anatomic center (or head CoG for rear-end impacts) in the laboratory reference (or in the head anatomic reference for rear-end impacts); AAy, AAx, AAz head angular accelerations in the head anatomic reference; RA resultant acceleration of the head anatomic center (or head CoG for rear-end impacts); AVy head angular velocity in the head anatomic reference.

Table 5. *Injury test conditions*

Source	N° of subjects	Tests	Velocity	End conditions[(1)]	Validation data[(2)]
(Nightingale *et al.* 1991)	6 C0-T1 6 C0-T1 6 C0-T1	Axial compression	0.045 m/s 0.02 m/s 0.01 m/s	Unconstrained Rot. constraint Full constraint	F, E, Ry F, E F, E
(Nightingale *et al.* 1997)	10 C0-T1	Head impact	Initial 3.2 m/s	Surface angle +15°, 0° and –15°	HF, NF
(Myers *et al.* 1991)	6 C0-T1 6 C2-T1	Axial torsion	500 °/s 500 °/s		T T

[(1)]Unconstrained: C0 rotation and translations (horizontal and axial) allowed; Rotation constraint: C0 horizontal and axial translations allowed; Full constraint: only axial translation allowed.

[(2)]F Peak axial load; E energy at failure; Ry head flexion; T torque to injury; HF head peak force; NF neck peak force.

3. Results

3.1. *Static behaviour simulations*

The model fits well with all the experimental values, reproducing main and coupled motions, for all directions of loading (see Table 6). Moreover, model functional units exhibit a neutral zone like experimental results do.

Table 6. *Model functional spinal unit main and coupled range of motions, under 2 N.m pure moment. Comparison with experimental (Watier 1997) mean results (standard deviations)*

	Flexion-extension		Lateral bending				Axial torsion			
	main motion Ry[(1)]		main motion Rx[(1)]		Coupled motion Rz[(1)]		main motion Rz[(1)]		Coupled motion Rx[(1)]	
	Model	Tests	M.	T.	M.	T.	M.	T.	M.	T.
C2/C3	10.6	7.3 (3.1)	12.7	8.7 (3.4)	6.3	6.5 (3.5)	6.8	9.5 (3.9)	4.7	6.5 (5.6)
C3/C4	9.6	10.6 (3.2)	12.6	6.7 (4.3)	6.0	4.3 (2.3)	8.6	10.8 (4.8)	4.3	5.9 (4.7)
C4/C5	12.9	13.8 (1.6)	12.3	10.5 (2.7)	6.8	5.9 (4.7)	9.0	12.3 (3.3)	5.2	6.6 (3.6)
C5/C6	9.2	13.4 (4.0)	15.3	11.2 (3.1)	3.2	5.5 (2.5)	9.9	9.0 (3.1)	5.9	6.5 (2.6)
C6/C7	10.6	10.8 (3.9)	10.8	8.6 (2.7)	2.9	3.2 (1.7)	8.6	5.6 (2.0)	5.1	3.8 (2.5)
C7/T1	6.1	6.4 (2.7)	4.8	5.7 (1.8)	0.9	1.9 (1.3)	4.7	5.7 (1.6)	2.2	3.4 (5.0)

[(1)]Ry sagittal plane rotation; Rx lateral bending rotation; Rz axial rotation; All values in degrees

3.2. *Kinematics simulations*

A visual representation of the simulations for the various impact conditions is presented in (Figure 3).

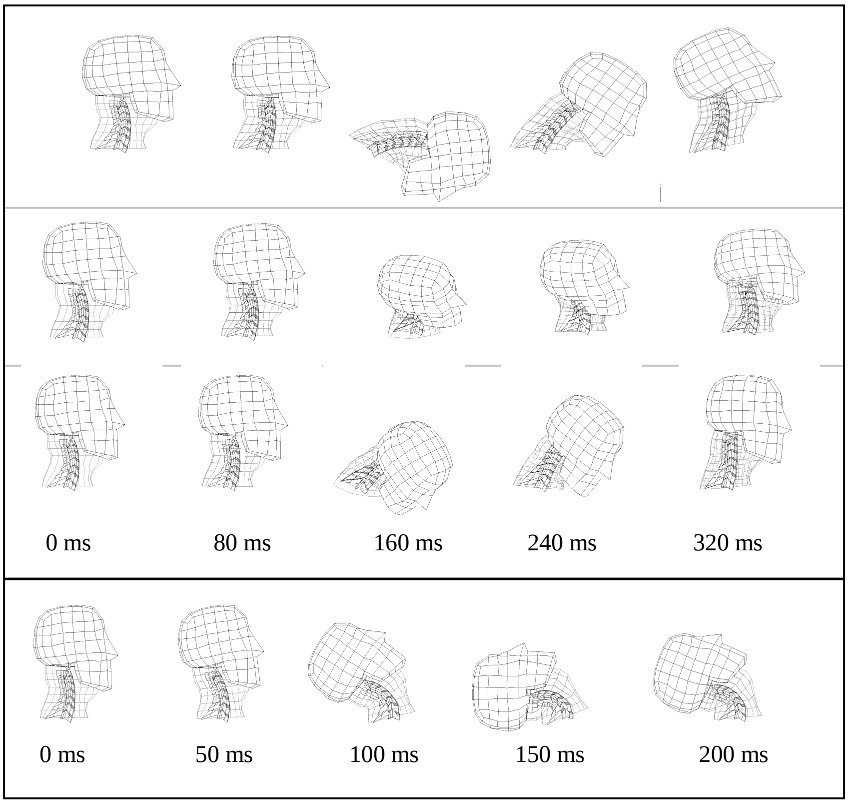

Figure 3. *Frontal, lateral, oblique and rear-end impact simulations. Muscles and soft tissues not represented*

3.2.1. *Frontal impacts* [1]

Model and experimental responses are in agreement for the frontal 15g impact (Figure 3) both for loading and unloading phases, although model vertical head displacement relative to T1 vertebra and head flexion are outside volunteer corridors after 250 ms. Model head linear and angular accelerations are well correlated during the 400 ms impact duration. Model responses during frontal impacts with different

1. For the ease of the reader, all results figures are compiled in an appendix.

severities (Table 7) are in general included into volunteer values. Particularly the tendency of increasing peak values with increase of severity is well reproduced by the model.

3.2.2. *Rear-end impacts*

Model and experimental responses during rear-end impacts are in good agreement (Figure 4) for the three impact velocities. Head displacements and rotations are well simulated and the model exhibits the initial S shape observed on human being. Relative vertebral rotations C0/C2, C2/C5, C5/T1 show a similar behaviour to experimental results (Bertholon *et al*., 2000).

Table 7. *Model responses for frontal impacts. Comparison with experimental (Ewing* et al.) *results (minimal-maximal volunteer values)*

Severity[1]	Peak head resultant acceleration (m/s^2)		Peak head angular acceleration (rad/s^2)		Peak head angular velocity (rad/s)	
	Model	Tests	Model	Tests	Model	Tests
6 g hosd	63.8	37.4 – 83.8	367	295 – 488	12.7	8.7 – 12.6
6 g lold	86.2	54.8 – 78	325	213 – 489	13.0	11.3 – 14.9
6 g hold	93.8	61.5 – 101.3	430	352 – 633	15.1	9.8 – 16.9
10 g hosd	158	69.9 – 175	847	446 – 1365	20.3	15.4 – 21.4
10 g lold	185	110 – 223	585	575 – 1209	23.3	18.7 – 26.4
10 g hold	184	158.7 – 235	875	900 – 1491	23.7	20.9 – 28.2
15 g hosd	183	145 – 274	1245	1217 – 2176	19.2	22.8 – 32.1
15 g lold	266	222 – 281	912	1466 – 1802	32.9	32.2 – 40.1
15 g hold	324	210 - 370	1215	1402 - 2666	31.5	29.5 – 41.5

[1]Sled acceleration profile: hosd high rate of onset - short duration; lold low rate of onset – long duration; hold high rate of onset - long duration.

Thus, during initial phase, the model head translates relative to the thorax without extension. In fact during this phase the model head is flexed relative to C2 vertebra. This phenomenon was observed on cadavers (Bertholon *et al*., 2000) and widely described in the literature (Grauer *et al*., 1997; Panjabi *et al*., 1998). Head linear and angular accelerations are similar with volunteers ones.

3.2.3. *Lateral and oblique impacts*

Model and experimental responses for lateral 7 g and oblique 10 g impact conditions are in good agreement (Figure 5) both for loading and unloading phases.

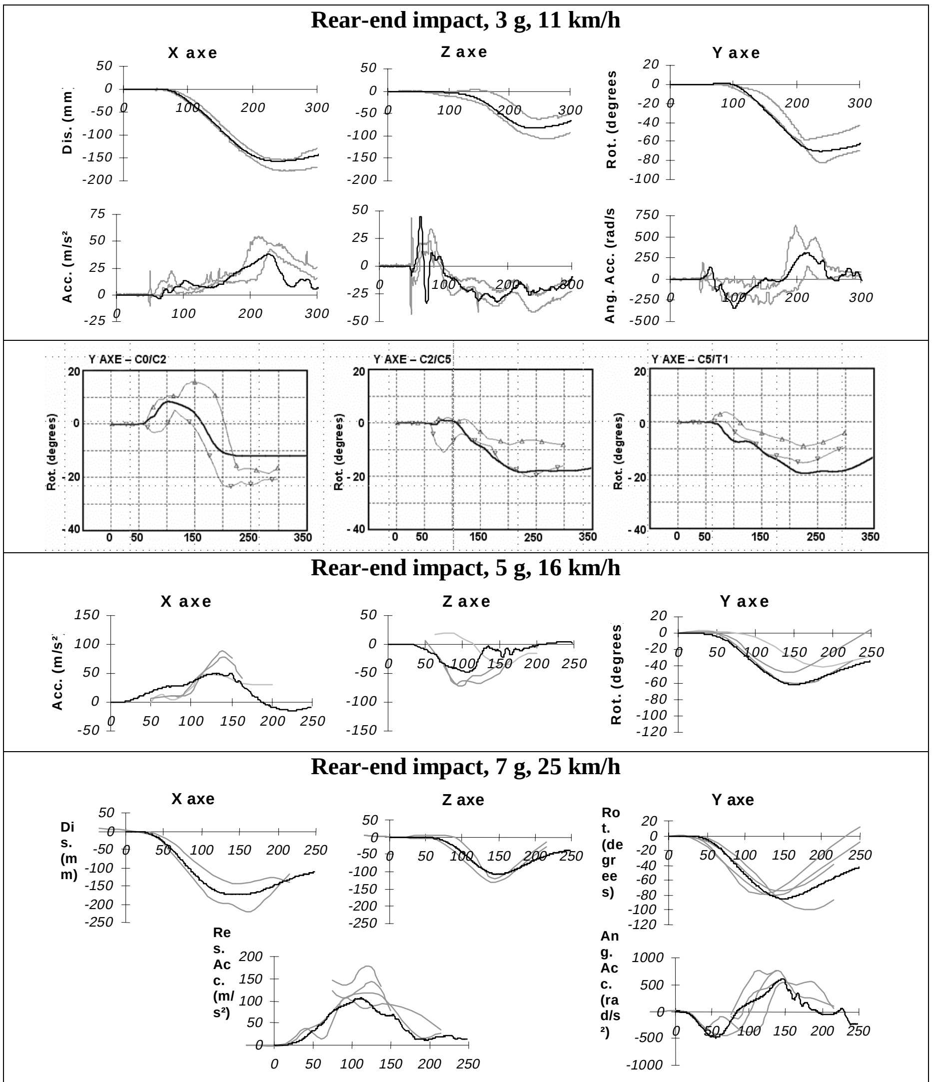

Model curves in black and test corridors in gray. Time, in ms, is in abscissa. Dis.: displacements of the head anatomic center (or head CoG for rear-end impacts) from T1 in the laboratory reference; Rot.: head (vertebras when specified) rotations in the laboratory reference; Acc.: accelerations of the head anatomic center (or head CoG for rear-end impacts) in the laboratory reference (or in the head anatomic reference for rear-end impacts); Ang. Acc.: head angular accelerations in the head anatomic reference; Res. Acc.: resultant acceleration of the head CoG.

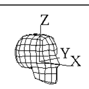

Figure 4. *Model responses for rear-end impacts*

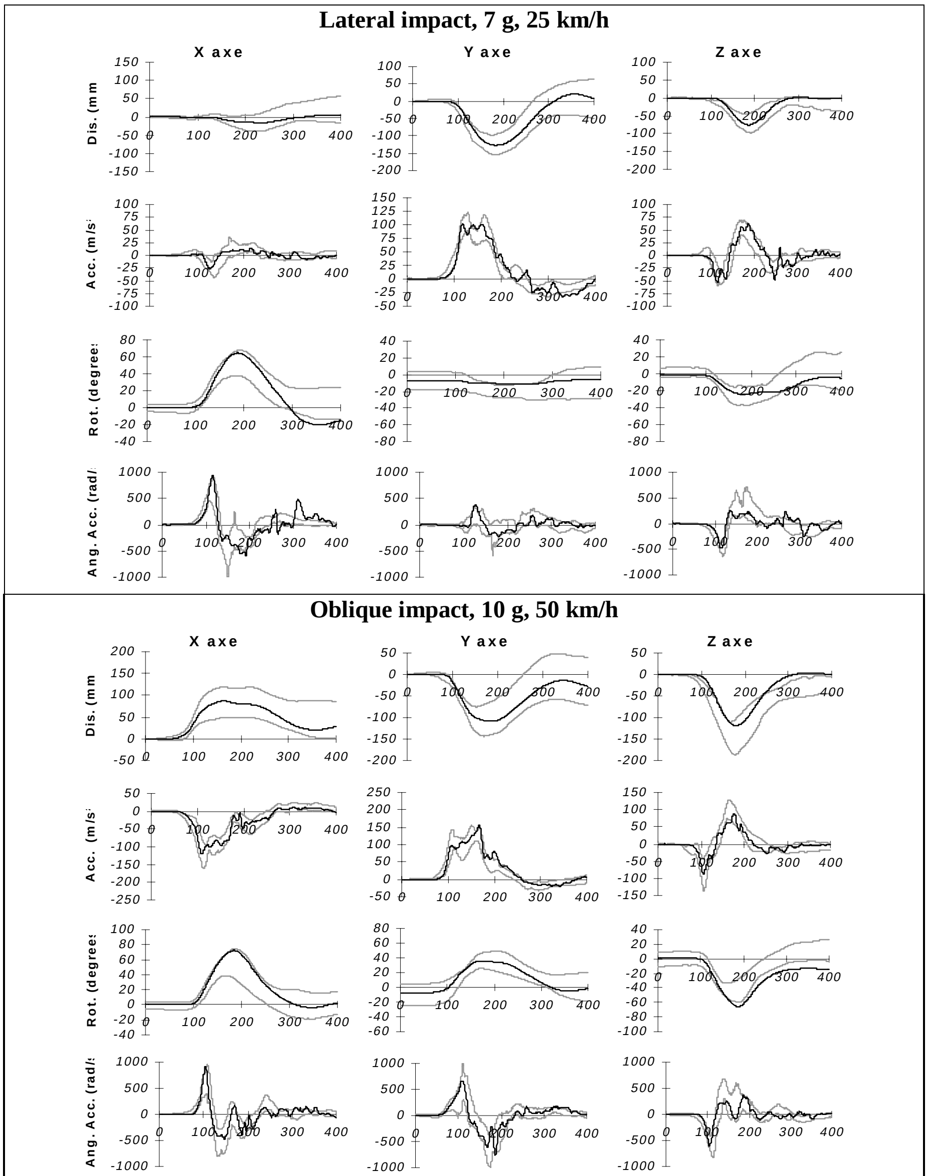

Model curves are black and test corridors are gray. Time, in ms, is in abscissa. Dis.: displacements of the head anatomic center from T1 in the laboratory reference; Rot.: head rotations calculated using Bryant's method of the head anatomic reference with respect to the laboratory reference; Acc.: accelerations of the head anatomic center in the laboratory reference; Ang. Acc.: head angular accelerations in the head anatomic reference.

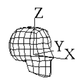

Figure 5. *Model responses for lateral and oblique impacts*

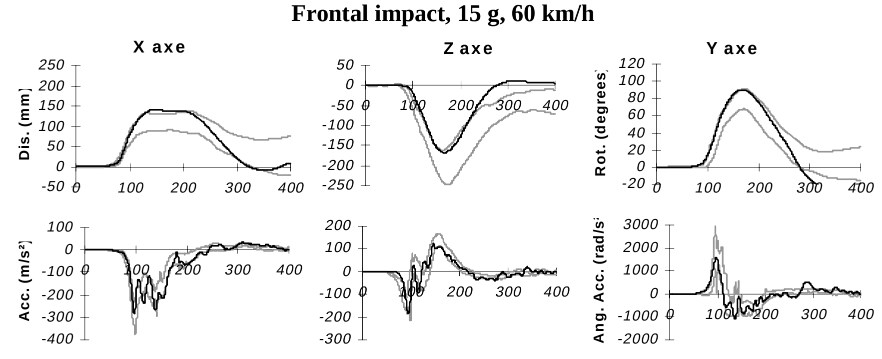

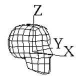

Model curves in black and test corridors in gray. Time, in ms, is in abscissa. Dis.: displacements of the head anatomic center (or head CoG for rear-end impacts) from T1 in the laboratory reference; Rot.: head rotations in the laboratory reference; Acc.: accelerations of the head anatomic center (or head CoG for rear-end impacts) in the laboratory reference (or in the head anatomic reference for rear-end impacts); Ang. Acc.: head angular accelerations in the head anatomic reference; Res. Acc.: resultant acceleration of the head CoG.

Figure 6. *Model responses for frontal impacts*

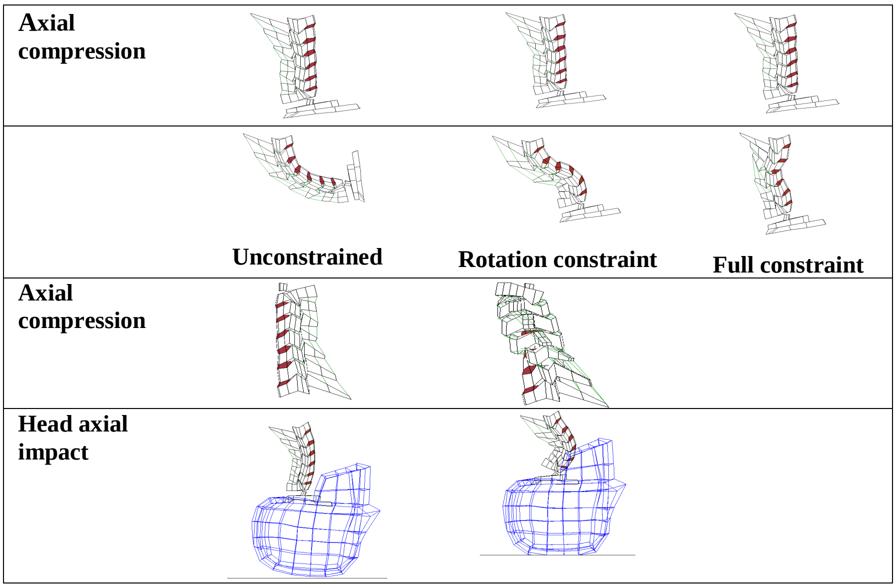

Figure 7. *Cervical spine injury test simulations*

For lateral impact, model head displacements relative to T1 vertebra are included into volunteer corridors during loading and rebound phases. Head rotations are also within corridors, although during rebound phase lateral bending rotation exceed volunteer ones. Model head linear and angular accelerations are well correlated during the 400 ms impact duration.

For oblique impact, model head displacements relative to T1 vertebra are included into volunteer corridors during loading and rebound phases. However, vertical displacement is slightly low and exceeds the corridor after 250 ms. Head rotations are also very close to corridors. Lateral bending rotation is rather high and flexion exceeds reasonably (8 %) volunteer corridor. Rebound rotations are identical to volunteer ones, except head flexion that stays quite above corridors. Model head linear and angular accelerations are well correlated during the 400 ms impact duration.

3.3. *Injury simulations*

3.3.1. *Cervical spine axial compression simulations*

Table 8 presents model and experimental results (Nightingale *et al.*, 1991) obtained during cervical spine compressions with three different end conditions (see Figure 7). Model results are taken at mean experimental failure displacement. For the three end conditions, mechanical model responses (peak axial loads, energy at failure and head flexion for unconstrained condition) are close to experimental values. Furthermore, during non-injury test simulation, none of the model criteria are exceeded and during injury test simulations model criteria corresponding to real injuries are exceeded. Thus, during rotation constraint test, articular capsules and posterior ligament model elongation at C6-C7 and C7-T1 levels are higher than tolerance values. These results correspond to bilateral facet dislocation and posterior ligamentous disruption observed experimentally at the same levels. Flexion moment at C7 functional unit level and extension moment at C5 functional unit level are also exceeded during simulation, corresponding to experimental change in cervical spine curvature between those levels. In a same manner, during full constraint test, model axial compression criteria are higher than tolerance values for all functional units, corresponding well to experimental vertebral fracture obtained at all cervical spine levels.

3.3.2. *Cervical spine axial torsion simulations*

Table 9 presents model and experimental results (Myers *et al.*, 1991) obtained during cervical spine torsion (see Figure 7). The simulations give identical results to experiments concerning torque to injury of whole or lower cervical spine. Moreover, model criteria allow identifying experimental injuries. Thus during whole cervical torsion, model axial torsion moment tolerance value is reached without any other model criterion exceeded. This result corresponds to systematic rotatory atlantoaxial facet dislocations obtained in vitro. During lower cervical spine torsion, model axial torsion moment criteria are exceeded at C5 and C7 levels and also right or left articular capsule elongation criteria for C4-C5, C5-C6 and C6-C7 levels. When the loading is continued a model unilateral facet dislocation appears at C5-C6 level. Figure 7 shows a representation of this phenomenon. Thus, experimental unilateral facet dislocations are reproduced with the model and at the same levels.

Table 8. *Comparison of model and tests (Nightingale* et al., *1991) results during cervical spine axial compressions. Mechanical responses and injuries*

End condition		Peak axial load (N)	Energy at failure (J)	Flexion (degrees)	Experimental injury and model criteria exceeded[(2)]
Uncons-Trained	Tests[(1)]	289 (81.4)	11.5 (6.5)	96 (7.3)	None
	Model	176	10.8	91.8	None
Rotation constraint	Tests[(1)]	1720 (1234)	26.8 (23.7)	-	1 BFD, IL and FL at C5-C6 level 1 BFD, IL and FL at C6-C7 level 4 BFD, IL and FL at C7-T1 level
	Model	1543	32.4	-	My C5 (-14.2 N.m) My C7 (+39.4 N.m) AC r. & l. at C6-C7 & C7-T1 levels IL & FL at C6-C7 & C7-T1 levels
Full constraint	Tests[(1)]	4810 (1286)	32.9 (12.8)	-	1 CF at C2 vertebra 2 CF at C3 vertebra 3 CF at C4 vertebra 3 CF at C5 vertebra 1 CF at C6 vertebra
	Model	5355	34.0	-	Fz C2 (-5354 N) Fz C5 (-4566 N), My C5 (+16.6 N.m) Fz C7 (-5328 N), My C5 (-22.0 N.m)

[(1)]Mean (standard deviation)

[(2)]BFD bilateral facet dislocation; IL interspinous ligament; FL flava ligament; My flexion – extension moment (peak value obtained, positive in flexion or negative in extension), AC articular capsule (r. right and l. left); CF vertebral body compression fracture; Fz axial loading (peak value obtained, positive in traction or negative in compression).

Table 9. *Comparison of model and tests (Myers* et al.*, 1991) results during cervical spine axial torsion. Mechanical responses and injuries*

Specimen		Torque to injury (N.m)	Experimental injury and model criteria exceeded(2)
Cervical spine (T1-C0)	Tests(1)	17.17 (5.13)	6 RFD at C1-C2 level
	Model	16.7	Mz C2 (22.4 N.m)
Lower cervical spine (T1-C2)	Tests(1)	21.03 (5.40)	2 UFD at C4-C5 level 1 UFD at C5-C6 level 3 UFD at C6-C7 level
	Model	23.4	Mz C5 (29.3 N.m) Mz C7 (28.0 N.m) AC r. at C6-C7 & C4-C5 levels AC l. at C5-C6 & C4-C5 levels IL at C6-C7 level

(1)Mean (standard deviation)

(2)RFD rotatory facet dislocation; Mz axial torsion moment (peak value obtained); UFD unilateral facet dislocation with posterior ligamentous disruption; AC articular capsule (r. right and l. left); IL interspinous ligament.

Table 10. *Comparison of model and tests (Nightingale* et al.*, 1997) results during head axial impact. Mechanical responses and injuries*

	Head peak force (N)	Neck peak force (N)	Experimental injury and model criteria exceeded(3)
Tests(1)	7977 (1795)	3426 (912)	Compression type injuries at C0-C2 level Compression extension type injuries at C3-C5 level Compression flexion type injuries at C6-T1 level
Model(2)	7744 10474 8887	3834 4888 4599	My C2 (+46 N.m), Fz C2 (-4593 N) My C5 (-44 N.m), Fz C5 (-4027 N) My C7 (+47 N.m), Fz C7 (-3919 N)

(1)Mean (standard deviation) for all surface angles.

(2)Values for each surface angle (+15°/0°/-15°).

(3)My flexion – extension moment (peak value obtained, positive in flexion or negative in extension); Fz axial loading (peak value obtained, positive in traction or negative in compression).

3.3.3. *Head axial impacts simulations*

Table 10 presents model and experimental results (Nightingale *et al.*, 1997) obtained during head axial impacts. A representation of model simulation with horizontal impact surface is given in Figure 7. Model results are similar to experimental ones concerning head peak force and quite higher concerning neck peak force. Cervical spine deformations obtained during experiments are also well reproduced with the model. Figure 7 presents the flexion of lower cervical spine (between C6 and T1) and extension of mid cervical spine (between C2 and C5). Model injury criteria are exceeded for flexion moment at C7 spinal unit level and for extension moment at C5 spinal unit level, plus for axial compression force at all spinal unit levels. Thus, “compression-flexion” type injuries of lower cervical spine, “compression-extension” type injuries of mid cervical spine and compression type injuries of upper cervical spine are well predicted with the model.

3.3.4. *Frontal impacts*

Frontal 15 g impacts with volunteers realized at the NBDL (Dauvilliers *et al.*, 1994) were duplicated with cadavers at Heidelberg University (Wismans *et al.*, 1987). Some kinematics and injury differences were found between volunteers and cadavers. These tests were simulated with alive (see kinematics validations above) and post mortem model muscle behaviours. Concerning head kinematics, model simulations show vertical displacement and flexion higher with post mortem muscle than with alive muscle, but similar accelerations. These results were the same than those observed during experiments. During experiments, none volunteer was injured but 8 of the 9 cadavers sustained injuries. Those injuries were: 1 T2 vertebral fracture, 9 hemorrhages in mid cervical or upper thoracic intervertebral disks and 3 strains in upper cervical spine joints. During model simulation with alive muscle, none of model injury criterion is exceeded corresponding to volunteer results. During model simulation with post mortem muscle, some model injury criteria are exceeded. Traction force criterion in C2 functional unit (+1620 N) exceeds tolerance value. This result can explain experimental upper cervical spine injuries. Moreover, flexion moment criterion in C7 functional unit is higher (+30.4 N.m) than the tolerance value. This result can explain experimental cervical and thoracic intervertebral disk injuries. Interspinous and flava ligament elongation criteria are also exceeded within the model, but injuries to these ligaments were not reported in cadaver autopsies.

4. Discussion

Understanding mechanisms of injury is of primary importance for improvement of protection devices, and a finite elements model can be of significant help providing it is relevant enough to bring to the light the main features of these injury mechanisms. That is the reason for the thorough evaluations that were performed.

Full model validation is difficult, mainly because of the lack of published data concerning the dynamic mechanical properties of some of the neck tissues. In order to assess the influence of these properties on the behaviour of the model, a sensitivity analysis had first been performed on the cervical spine model, using a 11-parameters, 2-levels Taguchi method (Bertholon, 1999). The influence of these parameters on the kinematics of the head was found to be depending on the impact direction, and the intervertebral disk parameters (short-time modulus E_0 and decay constant β) showed the most significant influence. However, as the model's behaviour had to be validated in multiple configurations, these parameters were not optimized for a particular kind of impact, and it is the volumic modelling of the soft tissues and muscles which proved to improve significantly the behaviour of the initial model. With these improvements, the kinematic results obtained with our model were similar to the volunteer and cadaver responses for all impact directions. Head displacements, rotations, linear and angular accelerations were coherent with experimental results during loading and rebound phases. The model reproduced well the initial head translation observed on subjects for all impact directions. Moreover, the model's local cervical kinematics in rear-end impact were compared to experimental results and showed a similar behaviour.

As for injury aspects, many mechanisms (typically whiplash injuries in rear-end impact) are not yet fully described. However the model rendered mechanical behaviour for experimentally existing injury tests with a good coherence: it was able to reproduce some cervical spine injury mechanisms, such as bilateral or unilateral facet dislocation and vertebral fracture. Injuries and injury locations were predicted, in a wide range of situations, and the differences between volunteers and cadavers results which were observed experimentally could be reproduced and explained thanks to the model.

As for other recent studies (Hasegawa 2004; Stemper *et al.* 2004), the extensive validation undertaken showed that an evaluation of the local behaviour of a model's cervical spine was important when considering mechanisms of injury analysis at this level. This could be performed for the case of the rear-end impact, but experimental results, assessing the spine behaviour at local level in various impact conditions, are needed in order to allow further validation of this kind of models. Further improvements could also be brought to the model: A finer modelling of the upper cervical spine would allow the assessment of specific injuries located at this level. The active component of the muscular system could be taken into account with activation parameters (reflex delay, activation level, muscles activated) for each impact (Van Der Horst *et al.* 1997). These improvements could contribute to explain some injury mechanisms, like in frontal impact with airbag, and allow to explore the effects of awareness of the impact and of subsequent strategies of muscular activation. Also, personalization of the model to other parts of population, like women and children, could be of great interest. Indeed, injury neck frequency has been shown to be higher for women (Temming *et al.*, 1998) and specific neck injuries appear for little children (Burdi *et al.*, 1969).

Nevertheless, the current model, even at this stage of its development, should be an invaluable tool in a wide field of applications where prevention of head and neck injury is necessary.

5. Conclusion

A finite element model of the human neck was developed. It considered a volumic representation for the main functional parts of cervical spine, muscles and soft tissues. Mechanical static and dynamic properties were derived from literature. Behaviour of passive alive muscles and post mortem muscles were differentiated.

The cervical spine was validated for omnidirectional static loading. Global head and neck kinematics were evaluated for all kind of automotive impacts (frontal, oblique, lateral and rear-end). Except minor differences, Head displacements, rotations and accelerations correlated well with experimental results. Furthermore, local vertebral rotations were in agreement with experimental results in the case of rear-end impacts.

Model injury criteria were proposed from literature data and computer simulations. These criteria are on one hand forces and moments passing through functional spinal units and on the other hand ligament elongations. Injury mechanisms for unilateral or bilateral facet dislocation and for compression fracture of vertebral body were reproduced or identified with the model. Furthermore, the model appeared to be able to discriminate the behaviour of volunteers and cadavers submitted to the same impact conditions, both concerning the kinematics and the injury patterns.

This model presents kinematics and injury behaviours consistent with the whole experiments available. It reproduces omnidirectional neck kinematics of an average size male occupant and allows prediction of cervical spine injury risks. Finally, it proves the feasibility of injury identification with a numerical model, and should help in the design of protection devices.

6. References

Becker E., “Measurement of Mass Distribution Parameters of Anatomical Segments”, *Proceedings of the 16th Stapp Car Crash Conference*, 1972, pp. 160-173.

Beier G., Schuller E., Schuck M., Ewing C., Becker E., Thomas D., “Center of gravity and moments of inertia of human heads”, *Proceedings of the 1980 International IRCOBI Conference*, 1980, pp. 218-228.

Bertholon N., Robin S., Skalli W., Le Coz J.-Y., Lavaste F., “Dynamic model of the human head-neck complex”, *Journal of Biomechanics*, 31 (Suppl. 1), 1998, pp. 44.

Bertholon N., Modélisation 3D du cou humain en situation de chocs omnidirectionnels,. Analyse cinématique et aspects lésionnels, PhD Thesis, ENSAM Paris, 1999.

Bertholon N., Robin S., Le Coz J. Y., Potier P., Lassau J. P., Skalli W., "Human head and cervical spine behaviour during low-speed rear-end impacts: PHMS sled tests with a rigid seat", *Proceedings of the 2000 International IRCOBI Conference*, 2000, pp. 265-289.

Burdi A., Huelke D., Snyder R., Lowrey G., "Infants and children in the adult world of automobile safety design; pediatric and anatomical considerations for design of child restraints", *Journal of Biomechanics*, 2, 1969, pp. 267-280.

Camacho D., Nightingale R., Robinette J., Vanguri S., Coates D., Myers B., "Experimental Flexibility Measurements for the Development of a computational Head-Neck Model Validated for Near-Vertex Head Impact", *Proceedings of the 41st Stapp Car Crash Conference*, 1997, pp. 473-486.

Chang H., Gilbertson L., Goel V., Winterbottom J., Clark C., Patwardhan A., "Dynamic response of the occipito-atlanto-axial (C0-C1-C2) complex in right axial rotation", *Journal of Orthopaedic Research*, Vol. 10, No. 3, 1992, pp. 446-453.

Dauvilliers F., Bendjellal F., Weiss M., Lavaste F., Tarrière C., "Development of a finite element model of the neck", *Proceedings of the 38th Stapp Car Crash Conference*, 1994, pp. 77-91.

De Jager M., Sauren A., Thunnissen J., Wismans J., "A Global and a Detailed Mathematical Model for Head-Neck Dynamics", *40th Stapp Car Crash Conf*, 1996, pp. 269-281.

Ewing C., Thomas D., Lustick L., Muzzy II I. W., Willems G., Majewski P., "The effect of duration, rate onset, and peak sled acceleration on the dynamic response of the human head and neck", *Proceedings of the 20th Stapp Car Crash Conference*, 1976, pp. 3-41.

Foust D., Chaffin D., Snyder R., Baum J., "Cervical range of motion and dynamic response and strength of cervical muscles", *Proceedings of the 17th Stapp Car Crash Conference*, 1973, pp. 285-308.

Goel V., Clark C., Gallaes K., King Liu Y., "Moment-rotation relationships of the ligamentous occipito-atlanto-axial complex", *Journal of Biomechanics*, Vol. 21, No. 8, 1988, pp. 673-680.

Goel V. K., Winterbottom J. M., Schulte K. R., Chang H., Gilbertson L. G., Pudgil A. G., Gwon J. K., "Ligamentous laxity across C0-C1-C2 complex, Axial torque-rotation characteristics until failure", *Spine* 15, 10, 1990, pp. 990-6.

Goubel F., Lensel-Corbeil G., *2003. Biomécanique éléments de mécanique musculaire*, Paris, France, Masson, 2003.

Grauer J. N., Panjabi M. M., Cholewicki J., Nibu K., Dvorak J., "Whiplash produces an S-shaped curvature of the neck with hyperextension at lower levels", *Spine* 22, (21), 1997, pp. 2489-94.

Halldin P., Brolin K., Kleiven S., Von Holst H., Jakobsson L., Palmertz C., Kleiven S., Von Holst H., "Investigation of conditions that affect neck compression-flexion injuries using numerical techniques", *Stapp Car Crash Journal*, 44, 2000.

Hasegawa J., "A study of neck soft tissue injury mechanisms during whiplash using human FE model", *Proceedings of the International IRCOBI Conference*, 2004, pp. 321-322.

Haut R., "Biomechanics of Soft Tissues, Accidental Injury", *Biomechanics and Prevention*, Springer-Verlag, 1993, pp. 224-246.

Kallieris D., Rizzetti A., Matten R., Thunnissen J., Philippens M., "Cervical Human Spine Loads During Traumatomechanical Investigations", *Proceedings of the International IRCOBI Conference*, 1996, pp. 89-106.

Kelley B., Lafferty J., Bowman D., Clark P., "Rhesus Monkey Intervertebral Disk Viscoelastic Response to Shear Stress", *Journal of Biomechanical Engineering*, 105, 1983, pp. 51-54.

Lizee E., Robin S., Song E., Bertholon N., Le Coz J. Y., Besnault B., Lavaste F., "Development of a 3D Finite Element Model of the Human Body", *Proceedings of the 42nd Stapp Car Crash Conference*, 1998, pp. 115-138.

McElhaney J., Stalnaker R., Estes M., Rose L., Strain rate sensitivity of certain biological materials, NASA Final Report for project N°SC-NsG-553/49-01-001, 1965.

McElhaney J., Paver J., McCrackin H., Maxwell M., "Cervical spine compression responses", *Proceedings of the 27th Stapp Car Crash Conference*, 1983, pp. 163-177.

Moroney S., Schultz A., Miller J., G. A., "Load-displacement properties of lower cervical spine motion segments", *Journal of Biomechanics*, Vol. 21, No. 9, 1988, pp. 769-779.

Myers B., McElhaney J., Doherty B., Paver J., Gray L., "The Role of Torsion in Cervical Spine Trauma", *Spine* 16, (8), 1991, pp. 870-874.

Myers B., Van Ee C., Camacho D., Woolley T., Best T., "On the structural and material properties of mammalian skeletal muscle and its relevance to human cervical impact dynamics", *Proceedings of the 39th Stapp Car Crash Conference*, 1995, pp. 203-214.

Myklebust J. B., Pintar F., Yoganandan N., Cusick J. F., Maiman D., Myers T. J., Sances A. Jr., "Tensile strength of spinal ligaments", *Spine* 13, (5), 1988, pp. 526-31.

National Library of Medicine, "Labeled visible human CD", *Research systems*, version 2.0, 1997.

Nightingale R., Myers B., McElhaney J., Doherty B., Richardson W., "The influence of end condition on human cervical spine injury mechanisms", *Proceedings of the 35th Stapp Car Crash Conference*, 1991, pp. 391-399.

Nightingale R., McElhaney J., Camacho L., Kleinberger M., Winkelstein B., Myers B., "The Dynamic Responses of the Cervical Spine: Buckling, End Condition, and Tolerance in Compressive Impacts", *Proceedings of the 41st Stapp Car Crash Conference*, 1997, pp. 451-471.

Panjabi M., Dvorak J., Duranceau J., Yamamoto I., Gerber M., Rauschning W., Bueff U., "Three-dimensional movements of the upper cervical spine", *Spine* 13, (7), 1988, pp. 726-730.

Panjabi M. M., Cholewicki J., Nibu K., Grauer J. N., Babat L. B., Dvorak J., "Mechanism of whiplash injury", *Clin Biomech* (Bristol, Avon), 13 (4-5), 1998, pp. 239-249.

Pintar F., Yoganandan N., Sances A., Reinartz J., Harris G., Larson S., “Kinematic and anatomical analysis of the human cervical spinal column under axial loading”. *Proceedings of the 33rd Stapp Car Crash Conference*, 1989, pp. 191-214.

Pintar F., Yoganandan N., Voo L., Cusick J., Maiman D., Sances A., “Dynamic characteristics of the human cervical spine”, *Proceedings of the 39th Stapp Car Crash Conference*, 1995, pp. 195-202.

Pintar F. A., Yoganandan N., Voo L., “Effect of age and loading rate on human cervical spine injury threshold”, *Spine* 23, (18), 1998, pp. 1957-62.

Prasad P., Kim A., Weerappuli D. P. V., “Biofidelity of Anthropomorphic Test Devices for Rear Impact”, *Proceedings of the 41st Stapp Car Crash Conference*, 1997, pp. 387-415.

Radioss, *User's manual version 4.2. Paris*, France, Mecalog sarl, 2001.

Robbins D., Schneider L., Snyder R., Pflug M. M. H., “Seated posture of vehicle occupants”, *Proceedings of the 27th Stapp Car Crash Conference*, 1983, pp. 129-224.

Shea M., Edwards W. T., White A. A., Hayes W. C., “Variations of stiffness and strength along the human cervical spine”, *Journal of Biomechanics*, Vol.24, No. 2, 1991, pp. 95-107.

Siegmund G. P., Myers B., Davis M. B., Bohnet H. F., Winkelstein B. A., “Human cervical motion segment flexibility and facet capsular ligament strain under combined posterior shear, extension and axial compression”, *Stapp Car Crash Journal*, 44, 2000, pp. 159-170.

Stemper B. D., Yoganandan N., Pintar F. A., “Validation of a head-neck computer model for whiplash simulation”, *Med Biol Eng Comput*, Vol. 42, No. 3, 2004, pp. 333-8.

Szabo T., Whelcher J., “Human Subject Kinematics and Electromyographic Activity During Low Speed Rear Impacts”, *Proceedings of the 40th Stapp Car Crash Conference*, 1996, pp. 295-315.

Temming J., Zobel R., “Frequency and risk of cervical spine distorsion injuries in passenger car accidents: significance of human factors data”, *Proceedings IRCOBI Conference*, 1998, pp. 219-233.

Thunnissen J., Wismans J., Ewing C., Thomas D., “Human volunteer head-neck response in frontal flexion: A new analysis”, *Proceedings of the 39th Stapp Car Crash Conference*, 1995, pp. 439-460.

Van Der Horst M., Thunnissen J., Happe R., Van Haaster R., Wismans J., “The Influence of Muscle Activity on Head-Neck Response During Impact”, *Proceedings of the 41st Stapp Car Crash Conference*, 1997, pp. 487-507.

Van Ee C., Chasse A., Myers B., “The Effect of Postmortem Time and Freezer Storage on the Mechanical Properties of Skeletal Muscle”, *Proceedings of the 42nd Stapp Car Crash Conference*, 1998, pp. 169-178.

Watier B., Etude expérimentale du rachis cervical: comportement mécanique *in vitro* et cinématique *in vivo*, PhD Thesis, ENSAM Paris, 1997.

White A., Panjabi M., *Clinical biomechanics of the spine*, Lippincott, 1990.

Winkelstein B. A., Nightingale R. W., Richardson W. J., Myers B. S., “Cervical facet joint mechanics: its application to whiplash injury”, *Stapp Car Crash Journal*, 43, 1999, pp. 243-252.

Wismans J., Philippens M., Van Oorchot E., Kallieris D., Matten R., “Comparaison of human volunteer and cadaver head-neck response in frontal flexion”, *Proceedings of the 31st Stapp Car Crash Conference*, 1987, pp. 1-13.

Yang K., Zhu F., Luan F., Zhao L., Begeman P., “Development of a Finite Element Model of the Human Neck”, *Proceedings of the 42nd Stapp Car Crash Conference*, 1998, pp. 195-205.

Yoganandan N., Pintar F., Butler J., Reinartz J., Sances A., Jr. Larson S. J., “Dynamic response of human cervical spine ligaments”, *Spine* 14, (10), 1989, pp. 1102-10.

Yoganandan N., Pintar F. A., Maiman D. J., Cusick J. F., Sances A., Jr. Walsh P. R., “Human head-neck biomechanics under axial tension”, *Med Eng Phys*, Vol. 18, No. 4, 1996, pp. 289-94.

Yoganandan N., Pintar F., Kumaresan S., Elhagediab A., “Biomechanical Assessment of Human Cervical Spine Ligaments”, *Proceedings of the 42nd Stapp Car Crash Conference*, 1998, pp. 223-236.